中國機械工程學刊第四十六卷第四期第 397~406 頁(民國一百一十四年)
Journal of the Chinese Society of Mechanical Engineers, Vol.46, No.4, pp397~406 (2025)

Structural Dynamic Analysis of Multistage Mounted Machine Foundation

Srihari Palli[*,*****], Rakesh Chandmal Sharma[**,***], Azad Duppala[*], Sunil Kumar Sharma[****,*****] and Neeraj Sharma[******]

Keywords：Raft, ANSYS, Machine 1, Machine 2, Natural frequency

ABSTRACT

Effective vibration isolation in machinery foundations is essential for reducing structure-borne noise and improving operational performance, particularly in naval, aerospace, and industrial applications. This study investigates the dynamic behavior and vibration isolation performance of a two-stage raft-mounted system. A nine-degree-of-freedom (DoF) mathematical model was developed, considering translational and rotational motions, and analyzed using MATLAB and ANSYS. Modal analysis identified the natural frequencies of the system, ranging from 5.91 Hz to 24.71 Hz, with harmonic analysis used to evaluate the system's response under dynamic excitation forces. The experimental setup, involving impact hammer testing and accelerometers, validated the numerical results, achieving close agreement attributed to real-world conditions such as imperfect boundary constraints. The model assumes negligible damping for simplicity, focusing on the elastic response of the system

INTRODUCTION

Raft foundations, often constructed as thick, reinforced slabs of concrete or metal, are commonly used to distribute loads from structures to the ground. Raft foundations, often constructed as thick, reinforced slabs of concrete or metal, are commonly used to distribute loads from structures to the ground. In both static structures and vibrating machinery, these foundations serve as essential components to prevent Raft foundations, often constructed as thick, reinforced slabs of concrete or metal, are commonly excessive motion, which can disrupt machine performance and create adverse conditions for nearby personnel. Structural vibration, caused by dynamic forces from engines, pumps, and compressors, is a key challenge in heavy machinery.

Studies on vibration reduction emphasize the need for foundations with tailored dynamic properties to withstand these forces effectively. Various approaches, including finite element analysis (FEA) and soil-structure interaction models, have been explored to predict how machine foundations respond to vibrations and to optimize their design accordingly (Valliappan and Hakam 2001; Barata 2019). Multistage raft-mounted systems are effective solutions for vibration isolation in machinery, offering enhanced damping and stiffness control compared to single-stage systems (Zhao and Chen 2008; Qiu et al. 2022). In such systems, a primary raft supports multiple machines, with the raft mounted on isolators to the foundation. Finite element analysis is recommended for foundation design to identify resonance conditions and maintain vibration amplitudes within acceptable limits (Jayarajan and Kouzer 2014). In metallurgical production, where greater foundation vibration is common, dynamic vibration dampers are critical. For heavy forging tools and manipulators, foundations are modeled as rigid bodies placed on a homogeneous elastic isotropic half-space (Evgeny et al. 2021). Mathematical modelling was widely used in the investigation to simulate the experimental model in vibration analysis of different static and dynamic structures (Al-Wakel et al. 2015; Liu et al. 2022). The findings show a reasonable correlation between the numerical model's predictions and those from the experimental model. To ensure satisfactory performance, carefully considered analysis and construction must be applied to structures

Paper Received July,2024. Revised January, 2025. Accepted February, 2025. Author for Correspondence: Rakesh Chandmal Sharma.

*Mechanical Engineering Department, Aditya Institute of Technology and Management, Tekkali, India (srihari.palli@gmail.com), (duppalaazadin@gmail.com)
**Mechanical Engineering Department, Graphic Era (Deemed to be University), Dehradun, India (rcsharmaiitr@gmail.com)
***Mechanical Engineering Department, Graphic Era Hill University), Dehradun, India
****School of Technology, Gati Shakti Vishwavidyalaya, Vadodara, India (sunilsharmaiitr@gmail.com)
*****Institute of Railway Vehicles and Railway Technology, "Friedrich List" Faculty of Transport and Traffic Sciences, Technische Universität Dresden, Dresden, Germany. (sunil_kumar.sharma@tu-dresden.de)
****** Production Engineering Department, National Institute of Technology Agartala, Tripura India (kkrneeraj@gmail.com)

supporting machines that generate dynamic loads. These highly complex systems must be reduced to mathematical (Guizani et al. 2022) and computational models (Sharma, Palli and Sharma 2023) that act similarly to the prototype structure-machine-soil system.

This paper focuses on analyzing the vibration response of a two-stage raft-mounted system, specifically examining the interaction between machine components on the raft and the foundation. To model this system, we develop a nine-degree-of-freedom (DoF) framework, which captures essential translational and rotational dynamics across multiple mounting stages. This model is analyzed using both MATLAB and ANSYS, with modal and harmonic analyses applied to determine the natural frequencies, mode shapes, and displacement responses under simulated dynamic loading.

MATHEMATICAL MODELING

Two-stage raft-mounted undamped vibration isolation

In the dynamic analysis of any machinery base, the number of model degrees of freedom (DoF's) is very important in determining many of the essential parameters of the system dynamics. In the current study, a model with nine degrees of freedom (DoF) is used, which describes the motion of translational and rotational components of the raft and machinery. This approach simplifies the analysis by focusing on vertical vibrations and neglecting the yaw rotation angle and the horizontal displacements (Xie et al. 2024). While this simplification may overlook certain horizontal or rotational movements, it enables a focused examination of the primary system behavior—vertical vibration response. The determination of 9 DoFs for the system was based on the speculation that vertical vibrations are most critical for vibration isolation efficiency. The two-stage raft-mounted vibration isolation system described here is depicted in Figure 1.

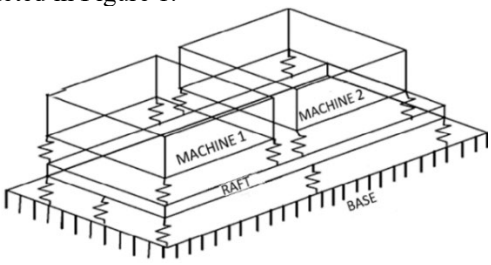

Figure 1. Two-stage raft-mounted isolation system

It consists of two machines, M1 and M2, mounted on a raft, which is in turn mounted on a rigid base. The system includes isolators positioned between the raft and the base, between the raft and machine M1, and between the raft and machine M2. These isolators have a specific stiffness value, denoted by $k_1, k_2, \ldots\ldots, k_{n_r}$ for the base-to-raft isolators, $k_{n_{r+1}} \ldots\ldots k_{n_{r+n1}}$ for the raft-to-M1 isolators, and $k_{n_r+n_1+1} \ldots\ldots k_{n_r+n_1+n_2}$ for the raft-to-M2 isolators. The raft's motion is defined by its translational displacement U_r and rotational angles θ_{rx} and θ_{ry} about its center of gravity (C.G.). Similarly, each machine (M1 and M2) experiences translational displacements U_1, U_2 and rotational displacements $\theta_{1x}, \theta_{1y}, \theta_{2x}, \theta_{2y}$ at their respective C.G.s. The isolators between the raft and the base are characterized by stiffness values $k_1, k_2, \ldots\ldots k_{n_r}$ while those between the raft and machine M1 are characterized by $k_{n_{r+1}} \ldots\ldots k_{n_{r+n1}}$, and those between the raft and machine M2 are represented by $k_{n_r+n_1+1} \ldots\ldots k_{n_r+n_1+n_2}$.

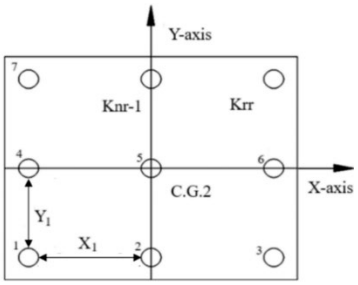

Figure 2. Raft with raft isolators.

Raft Isolators

$$F_1 = k_i\left(U_r + y_1\theta_{rx} + x_1\theta_{ry}\right) \quad (1)$$

$$F_2 = k_i\left(U_r + y_2\theta_{rx} + x_2\theta_{ry}\right) \quad (2)$$

$$F_{n_r} = k_{n_r}\left(U_r + y_{n_r}\theta_{rx} + x_{n_r}\theta_{ry}\right) \quad (3)$$

Machine M1 Isolators

$$F_{n_r+1} = k_{n_r+1}\left(U_1 + B_{n_r+1}\theta_{1x} + A_{n_r+1}\theta_{1y}\right) - \left(U_r + y_{n_r+1}\theta_{rx} + x_{n_r+1}\theta_{ry}\right) \quad (4)$$

$$F_{n_r+n_1} = k_{n_r+n_1}\left(U_1 + B_{n_r+n_1}\theta_{1x} + A_{n_r+n_1}\theta_{1y}\right) - \left(U_r + y_{n_r+n_1}\theta_{rx} + x_{n_r+n_1}\theta_{ry}\right) \quad (5)$$

Machine M2 Isolators

$$F_{n_r+n_1+1} = k_{n_r+n_1+1}\left(U_2 + D_{n_r+n_1+1}\theta_{2x} + C_{n_r+n_1+1}\theta_{2y}\right) - \left(U_r + y_{n_r+n_1+1}\theta_{rx} + x_{n_r+n_1+1}\theta_{ry}\right) \quad (6)$$

$$F_{n_r+n_1+n_2} = k_{n_r+n_1+n_2}\left(U_2 + D_{n_r+n_1+n_2}\theta_{2x} + C_{n_r+n_1+n_2}\theta_{2y}\right) - \left(U_r + y_{n_r+n_1+n_2}\theta_{rx} + x_{n_r+n_1+n_2}\theta_{ry}\right) \quad (7)$$

The positions of the raft isolators are variable which are defined in the X-Y Cartesian coordinate system with respect to the C.G. of the raft, as shown in Figure 2. The X and Y coordinates of the isolators are labelled as $x_1, x_2 \ldots\ldots x_{n_r}$, $x_{n_{r+1}} \ldots\ldots\ldots$, $x_{n_{r+n_1}}$, $x_{n_{r+n_1+1}} \ldots\ldots\ldots x_{n_{r+n_1+n_2}}$ and y_1, $y_2 \ldots\ldots y_{n_r}$, $y_{n_{r+1}} \ldots\ldots\ldots, y_{n_{r+n_1}}$, $y_{n_{r+n_1+1}} \ldots\ldots\ldots y_{n_{r+n_1+n_2}}$. For machine M1, the isolators are defined in the A-B

coordinate system, with isolator coordinates A_i and B_i corresponding to the isolator stiffness values k_i. For machine M2, the isolators are defined in the C-D coordinate system, with isolator coordinates C_i and D_i, corresponding to the stiffness values k_i as well. The forces acting on the isolators in the system are given from Eq (1-7). It is assumed that machines and raft have three degrees of freedom, translation (U) and rotations θ_x and θ_y and both machines and raft are rigid.

Equations of Motion

The equations of motion describe the dynamics of the raft and machines within the system, accounting for forces in the isolators and moments of inertia. The equation of motion for the bounce of the raft is given by Eq. (8).

$$M_r \ddot{U}_r + \sum_{i=1}^{n_t} k_i u_r + \sum_{n_r+1}^{n_r+n_1} -k_i u_1 + \sum_{i=n_r+n_1+1}^{n_t} -k_i u_2 + \sum_{i=1}^{n_t} k_i y_i \theta_{rx} + \sum_{i=1}^{n_t} k_i x_i \theta_{ry} + \sum_{i=n_r+1}^{n_r+n_1} -k_i B_i \theta_{1x} + \sum_{i=n_r+1}^{n_r+n_1} -k_i A_i \theta_{1y} + \sum_{i=n_r+n_1+1}^{n_t} -k_i D_i \theta_{2x} + \sum_{i=n_r+n_1+1}^{n_t} -k_i C_i \theta_{2y} = 0 \quad (8)$$

n_t = Total number of isolators in the system= $n_r + n_1 + n_2$. The equation of motion for the bounce of machine 1 is presented in Eq. (9).

$$M_1 \ddot{U}_1 + \sum_{i=n_r+1}^{n_r+n_1} -k_i u_r + \sum_{n_r+1}^{n_r+n_1} k_i u_1 + \sum 0u_2 + \sum_{i=n_r+1}^{n_r+n_1} -k_i y_i \theta_{rx} + \sum_{i=n_r+1}^{n_r+n_1} -k_i x_i \theta_{ry} + \sum_{i=n_r+1}^{n_r+n_1} k_i B_i \theta_{1x} + \sum_{i=n_r+1}^{n_r+n_1} k_i A_i \theta_{1y} + \sum_{i=n_r+n_1+1}^{n_t} 0\theta_{2x} + \sum_{i=n_r+n_1+1}^{n_t} 0\theta_{2y} = 0 \quad (9)$$

The equation of motion for the bounce of machine 2, roll of raft, pitch of raft, roll of machine 1, pitch of machine 1, roll of machine 2 and pitch of machine 2 is outlined in Eq. (10), (11), (12), (13), (14), (15) and (16) respectively.

$$M_2 \ddot{U}_2 + \sum_{i=n_r+n_1+1}^{n_t} -k_i u_r + \sum_{n_r+1}^{n_r+n_1} 0u_1 + \sum_{i=n_r+n_1+1}^{n_t} k_i u_2 + \sum_{i=n_r+n_1+1}^{n_t} -k_i y_i \theta_{rx} + \sum_{i=n_r+n_1+1}^{n_t} -k_i x_i \theta_{ry} + \sum_{i=n_r+1}^{n_r+n_1} 0\theta_{1x} + \sum_{i=n_r+1}^{n_r+n_1} 0\theta_{1y} + \sum_{i=n_r+n_1+1}^{n_t} k_i D_i \theta_{2x} + \sum_{i=n_r+n_1+1}^{n_t} k_i C_i \theta_{2y} = 0 \quad (10)$$

$$I_{rx} \ddot{\theta}_{rx} + \sum_{i=1}^{n_t} k_i y_i u_r + \sum_{n_r+1}^{n_r+n_1} -k_i y_i u_1 + \sum_{i=n_r+n_1+1}^{n_t} -k_i y_i u_2 + \sum_{i=1}^{n_t} k_i y_i^2 \theta_{rx} + \sum_{i=1}^{n_t} k_i x_i y_i \theta_{ry} + \sum_{i=n_r+1}^{n_r+n_1} -k_i B_i y_i \theta_{1x} + \sum_{i=n_r+1}^{n_r+n_1} -k_i A_i y_i \theta_{1y} + \sum_{i=n_r+n_1+1}^{n_t} -k_i D_i y_i \theta_{2x} + \sum_{i=n_r+n_1+1}^{n_t} -k_i C_i y_i \theta_{2y} = 0 \quad (11)$$

$$I_{ry} \ddot{\theta}_{ry} + \sum_{i=1}^{n_t} k_i x_i u_r + \sum_{n_r+1}^{n_r+n_1} -k_i x_i u_1 + \sum_{i=n_r+n_1+1}^{n_t} -k_i x_i u_2 + \sum_{i=1}^{n_t} k_i x_i y_i \theta_{rx} + \sum_{i=1}^{n_t} k_i x_i^2 \theta_{ry} + \sum_{i=n_r+1}^{n_r+n_1} -k_i B_i x_i \theta_{1x} + \sum_{i=n_r+1}^{n_r+n_1} -k_i A_i x_i \theta_{1y} + \sum_{i=n_r+n_1+1}^{n_t} -k_i D_i x_i \theta_{2x} + \sum_{i=n_r+n_1+1}^{n_t} -k_i C_i x_i \theta_{2y} = 0 \quad (12)$$

$$I_{1x} \ddot{\theta}_{1x} + \sum_{n_r+1}^{n_r+n_1} -k_i B_i u_r + \sum_{n_r+1}^{n_r+n_1} k_i B_i u_1 + \sum 0u_2 + \sum_{i=n_r+1}^{n_r+n_1} -k_i y_i B_i \theta_{rx} + \sum_{i=n_r+1}^{n_r+n_1} -k_i x_i B_i \theta_{ry} + \sum_{i=n_r+1}^{n_r+n_1} k_i B_i^2 \theta_{1x} + \sum_{i=n_r+1}^{n_r+n_1} k_i A_i B_i \theta_{1y} + \sum_{i=n_r+n_1+1}^{n_t} 0\theta_{2x} + \sum_{i=n_r+n_1+1}^{n_t} 0\theta_{2y} = 0 \quad (13)$$

$$I_{1y} \ddot{\theta}_{1y} + \sum_{n_r+1}^{n_r+n_1} -k_i A_i u_r + \sum_{n_r+1}^{n_r+n_1} k_i A_i u_1 + \sum 0u_2 + \sum_{i=n_r+1}^{n_r+n_1} -k_i y_i A_i \theta_{rx} + \sum_{i=n_r+1}^{n_r+n_1} -k_i y_i A_i \theta_{ry} + \sum_{i=n_r+1}^{n_r+n_1} k_i A_i B_i \theta_{1x} + \sum_{i=n_r+1}^{n_r+n_1} k_i A_i^2 \theta_{1y} + \sum_{i=n_r+n_1+1}^{n_t} 0\theta_{2x} + \sum_{i=n_r+n_1+1}^{n_t} 0\theta_{2y} = 0 \quad (14)$$

$$I_{2x} \ddot{\theta}_{2x} + \sum_{n_r+n_1+1}^{n_t} -k_i B_i u_r + \sum 0u_1 + \sum_{n_r+n_1+1}^{n_t} k_i B_i u_2 + \sum_{i=n_r+n_1+1}^{n_t} -k_i y_i B_i \theta_{rx} + \sum_{i=n_r+n_1+1}^{n_t} -k_i x_i B_i \theta_{ry} + \sum_{i=n_r+1}^{n_r+n_1} 0\theta_{1x} + \sum_{i=n_r+1}^{n_r+n_1} 0\theta_{1y} + \sum_{i=n_r+n_1+1}^{n_t} k_i B_i^2 \theta_{2x} + \sum_{i=n_r+n_1+1}^{n_t} k_i A_i B_i \theta_{2y} = 0 \quad (15)$$

$$I_{2y} \ddot{\theta}_{2y} + \sum_{n_r+n_1+1}^{n_t} -k_i A_i u_r + \sum 0u_1 + \sum_{n_r+n_1+1}^{n_t} k_i A_i u_2 + \sum_{i=n_r+n_1+1}^{n_t} -k_i y_i A_i \theta_{rx} + \sum_{i=n_r+n_1+1}^{n_t} -k_i x_i A_i \theta_{ry} + \sum_{i=n_r+1}^{n_r+n_1} 0\theta_{1x} + \sum_{i=n_r+1}^{n_r+n_1} 0\theta_{1y} + \sum_{i=n_r+n_1+1}^{n_t} k_i A_i B_i \theta_{2x} + \sum_{i=n_r+n_1+1}^{n_t} k_i A_i^2 \theta_{2y} = 0 \quad (16)$$

In the mathematical modeling, there are 6 raft isolators, 4 isolators associated with machine 1 (M-1), and 4 isolators associated with machine 2 (M-2). Therefore, the total number of isolators, is denoted as n_t= 14, which is the sum of the raft isolators n_r= 6, the machine 1 isolators n_1= 4, and the machine 2 isolators n_2= 4. These values can be substituted into the system of equations i.e., Eq. (8) to Eq. (16) as described in the model.

Table 1. Mass and inertial parameters.

	M-1	M-2	Raft
Mass (kg)	35	35	34
Mass Moment of Inertia, Ix (kg m^2)	0.271	0.271	0.032
Mass Moment of Inertia, Iy (kg m^2)	0.271	0.271	0.061

Table 2. Location of isolators for two-stage rafted system (distances in meters).

Isolator	Relative to C.G. of machine 1	Relative to C.G. of machine 2	Relative to C.G. of Raft

	A_i	B_i	C_i	D_i	x_i	y_i
1					-0.4	-0.292
2					0	-0.292
3					0.4	-0.292
4					-0.4	0.292
5					0	0.292
6					0.4	0.292
7	-0.1	-0.1			-0.341	-0.1
8	0.1	-0.1			-0.141	-0.1
9	-0.1	0.1			-0.341	0.1
10	0.1	0.1			-0.141	0.1
11			-0.1	-0.1	0.141	-0.1
12			0.1	-0.1	0.341	-0.1
13			-0.1	0.1	0.141	0.1
14			0.1	0.1	0.341	0.1

The specific values of the masses (M), moments of inertia (I), location of isolators, and stiffness of isolators are listed in Tables 1, 2, and 3, respectively. These parameters are crucial for the numerical solution of the equations and for analyzing the dynamic behavior of the system.

Table 3. Stiffness of isolators.

	Notations	Value
Raft Isolators	$K_{1,2,3,4,5,6}$	68148 N/m
Machine-1 Isolators	$K_{7,8,9,10}$	18572.51 N/m
Machine-2 Isolators	$K_{11,12,13,14}$	15679.27 N/m

ANALYSIS OF THE MATHEMATICAL MODEL

Natural frequencies and mode shapes (Analytical)

The mathematical model is analyzed using MATLAB to determine the natural frequencies of the raft mounting system. In free-free conditions, no constraints are applied to the model. This is done so that the results obtained from computational analysis can be compared with experimental eigenvalue analysis and ANSYS eigenvalue analysis. Figure 3 displays the relationship between amplitude and degrees of freedom. Table 4 shows the natural frequencies of the system obtained from MATLAB code.

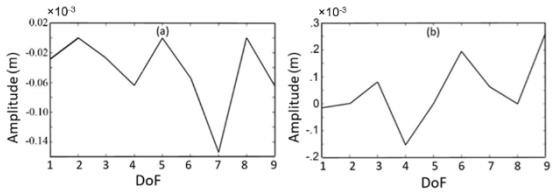

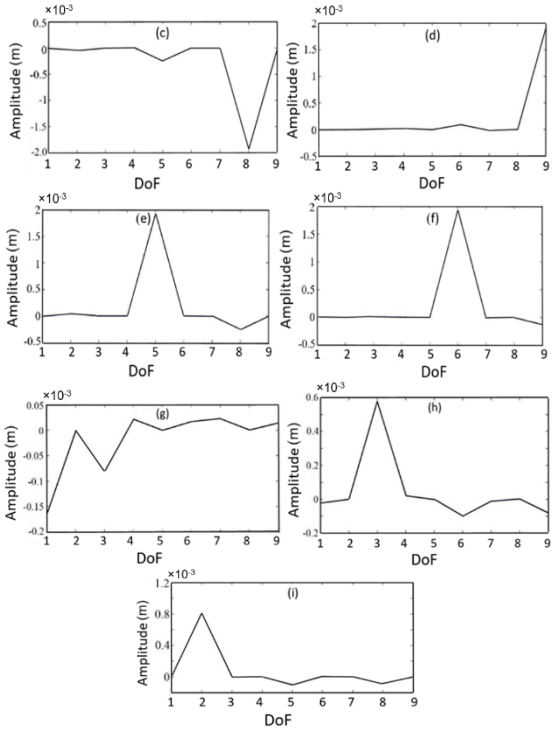

Figure 3. Amplitude Vs DoF for mode frequency from mode 1 to mode 9 (a) 5.9243 Hz (b) 6.4595 Hz (c) 7.7285 Hz (d) 7.7855 Hz (e) 8.3797 Hz (f) 8.4205 Hz (g) 20.4909 Hz (h) 22.0222 Hz (i) 24.7151 Hz.

Table 4. Natural frequencies and corresponding mode shapes of raft mounting system

Orders	**Value of frequency (Hz)**	**Vibration mode**
1	5.9243	M1 Bounce
2	6.4595	M2 Bounce
3	7.7285	M1 Rolling
4	7.7855	M1 Pitching
5	8.3797	M2 Rolling
6	8.4205	M2 Pitching
7	20.4909	Raft Bounce
8	22.0222	Raft Pitching
9	24.7151	Raft Rolling

Harmonic Response Analysis using MATLAB

The mode superposition method of harmonic analysis is performed on raft mounted isolation system in fixed conditions. In this analysis, a load of 1000 N is applied on (i) on Machine-1 only (Figure 4) (ii) on Machine-2 only (Figure 5) (iii) on two Machines (Figure 6). Frequency response of Raft, Machine-1 and Machine-2 are taken for these conditions. Responses are plotted in the semi-logarithmic graph; the x-axis shows the frequency and units' rad/sec; the y-axis shows the amplitude (responses) and units dB.

$$dB = 20 \log_{10} Response \quad (17)$$

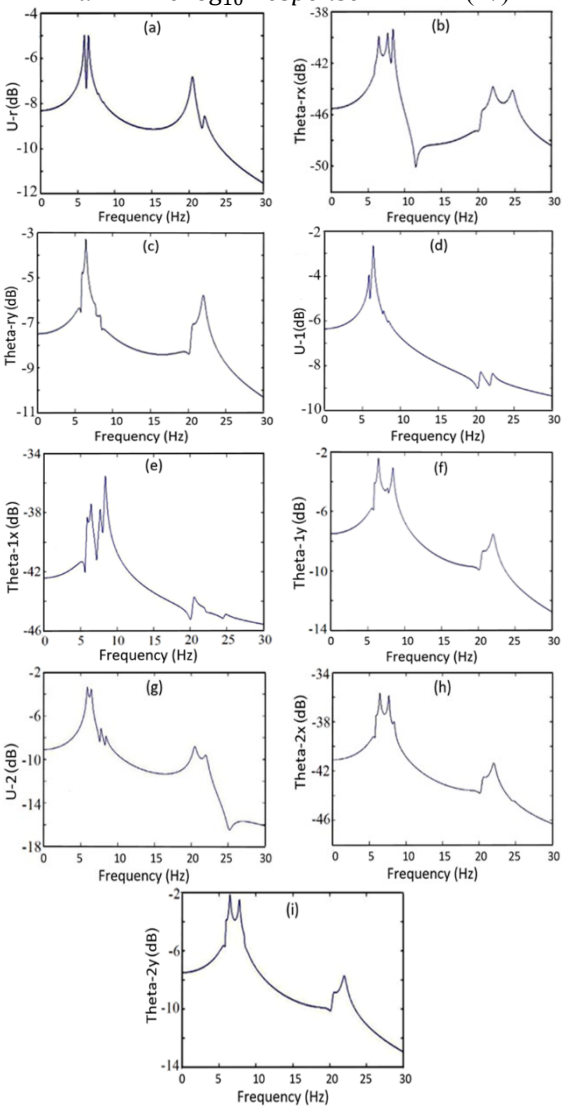

Figure 4. Frequency response of Raft: Bounce (a), Roll (b), Pitch (c), Machine-1: Bounce (d), Roll (e), Pitch (f) and Machine-2: Bounce (g), Roll (h), Pitch (i); when Machine-1 having excitation force (Analytical).

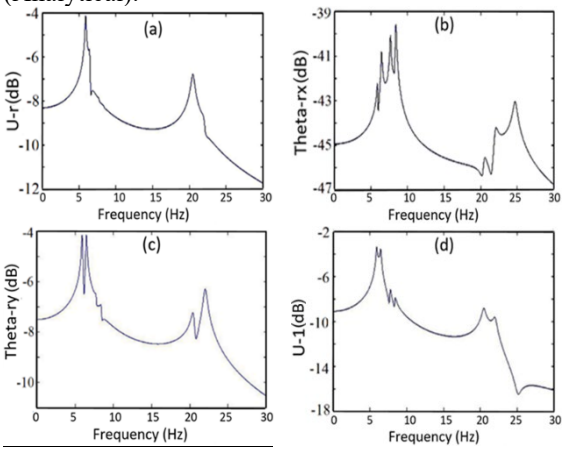

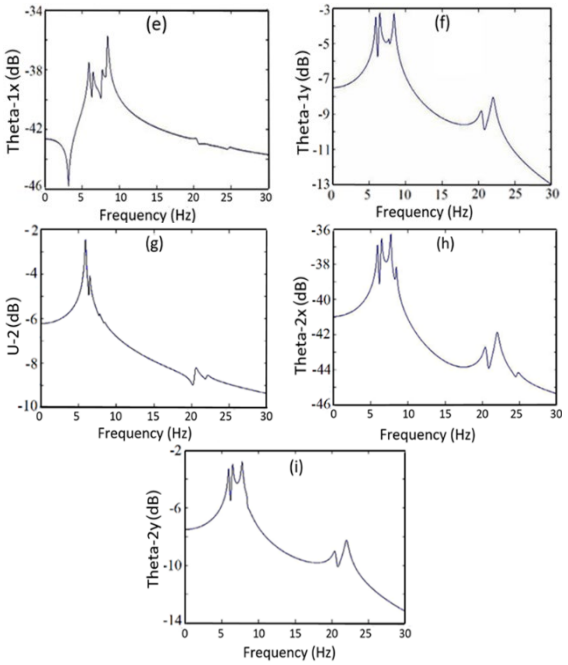

Figure 5. Frequency response of Raft: (a) Bounce (b) Roll (c) Pitch, Machine-1: (d) Bounce (e) Roll (f) Pitch and Machine-2: (g) Bounce (h) Roll (i) Pitch when; Machine-2 having excitation force (Analytical).

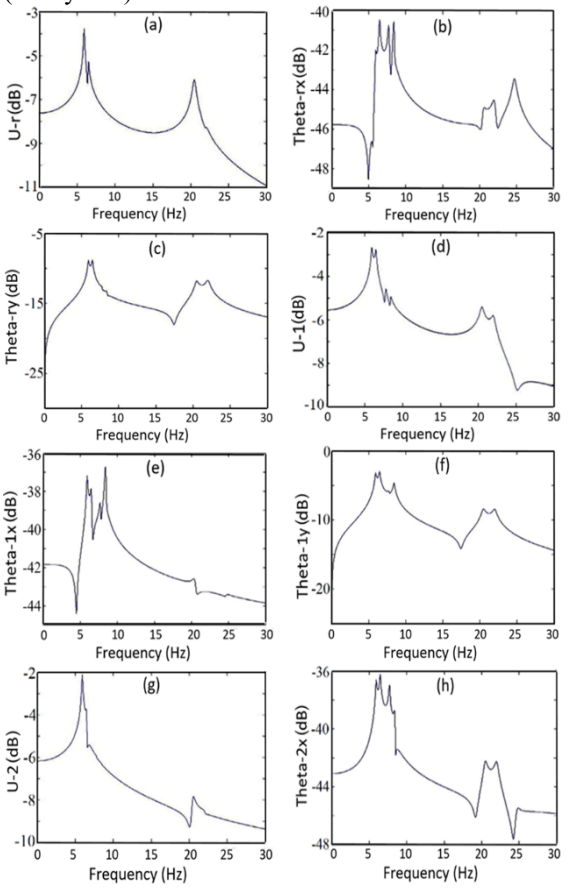

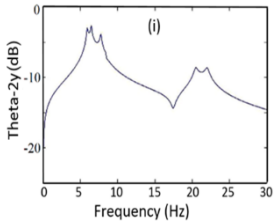

Figure 6. Frequency response of Raft: (a) Bounce (b) Roll (c) Pitch, Machine-1: (d) Bounce (e) Roll (f) Pitch and Machine-2: (g) Bounce (h) Roll (i) Pitch; when Machine-1 and Machine-2 having excitation force (Analytical).

Maximum and minimum amplitudes at natural frequencies of the raft-mounted system from mathematical analysis are listed in Table 5.

Table 5. Maximum and minimum amplitudes of raft system at mode frequencies (Analytical).

Mode Number	Maximum Displacement (m)	Minimum Displacement (m)
1	0.0297	-0.0247
2	0.0590	-0.0247
3	9.2490×10^{-17}	-4.3418×10^{-17}
4	0.0227	-0.0309
5	1.0383×10^{-17}	-8.4969×10^{-16}
6	0.0317	-0.0403
7	0.0118	-0.0108
8	2.013×10^{-18}	-1.4650×10^{-18}
9	0.0089	-0.0137

FINITE ELEMENT ANALYSIS USING ANSYS

Natural frequencies and mode shapes using ANSYS

Modal analysis is carried out using ANSYS to investigate the dynamic characteristics of the two-stage isolation system. In the two-stage system of isolation, a total of 14 spring elements have been used, wherein the foundation, raft and mounts have been simplified to three spring elements. The first stage of mounts connects the base and the raft whereas the second stage connects the raft to the prime movers. To realize the FEM, a hybrid of elements was utilized, so that there is a balance between computation time and detail level for the representation of the physical configuration. The rigid foundation was modelled using the MPC 184 beam link element while the parts that rotate, such as machines were modelled using the MPC 184 joint element. For the isolation system, the combination of COMBIN14 elements was used to model springs and dampers. This meshing strategy was selected to balance computational efficiency with the level of detail required for an accurate representation of the system. Following the approach of the MATLAB model, both the raft and the machines were treated as rigid bodies in the FEM model, and the geometry and stiffness parameters of the isolators were kept consistent.

This assumption ensured that the FEM model and MATLAB model were directly comparable, producing similar results while focusing on the primary objective of evaluating the vibrational behavior of the system with two-stage isolation.

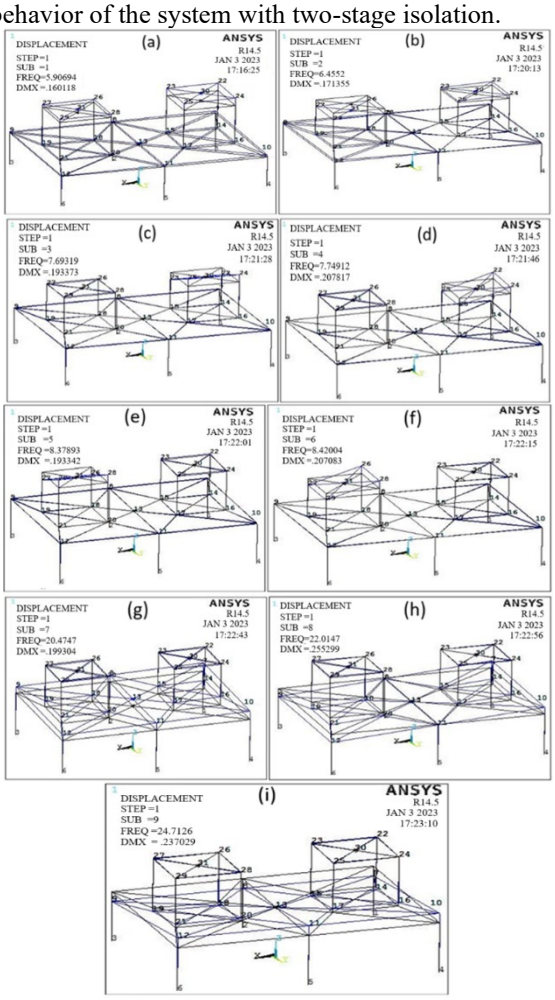

Figure 7. Mode shape corresponding to (a) bounce M1 bounce (b) M2 Bounce (c) M1 Rolling (d) M1 Pitching (e) M2 Rolling (f) M2 Pitching (g) Raft Bounce (h) Raft Pitching (i) Raft Rolling.

The results of the modal analysis, including the modal frequencies, are summarized in Table 6, while the corresponding mode shapes are displayed in Figure 7. These computational results from ANSYS are then compared with results obtained from MATLAB and experimental modal analysis, providing a comprehensive evaluation of the system's dynamic performance.

Table 6. Natural frequencies and corresponding mode shapes (ANSYS).

Orders	Value of frequency (Hz)	Vibration mode
1	5.9069	M1 Bounce
2	6.4554	M2 Bounce
3	7.6932	M1 Rolling
4	7.7491	M1 Pitching
5	8.3789	M2 Rolling
6	8.4200	M2 Pitching
7	20.475	Raft Bounce
8	22.015	Raft Pitching
9	24.713	Raft Rolling

Harmonic analysis using ANSYS

Definition of harmonic analysis: any sustained cyclic loads will produce a sustained cyclic response in a structural system. Harmonic response analysis gives the ability to predict the sustained dynamic behavior of any structure. It determines the steady state response of a linear structure to loads that vary sinusoidal with time. This calculates the structure's response at several frequencies and obtains a graph of some response quantity versus frequency. The two-stage isolation system is modelled with the foundation, raft, and mounts as springs and base. The first stage of mounts connects the foundation and raft. The second stage of mounts connects the raft and machines. The mounts are modelled using spring elements. The total spring elements on two-stage isolation are 14. The mode Superposition method of Harmonic analysis is performed on Raft mounted isolation system in fixed conditions. In this analysis, a load of 1000 N is applied on (i) Machine-1 only (Figure 8) (ii) Machine-2 only (Figure 9) (iii) two Machines (Figure 10). Frequency response of Raft, Machine-1 and Machine-2 are taken for these conditions.

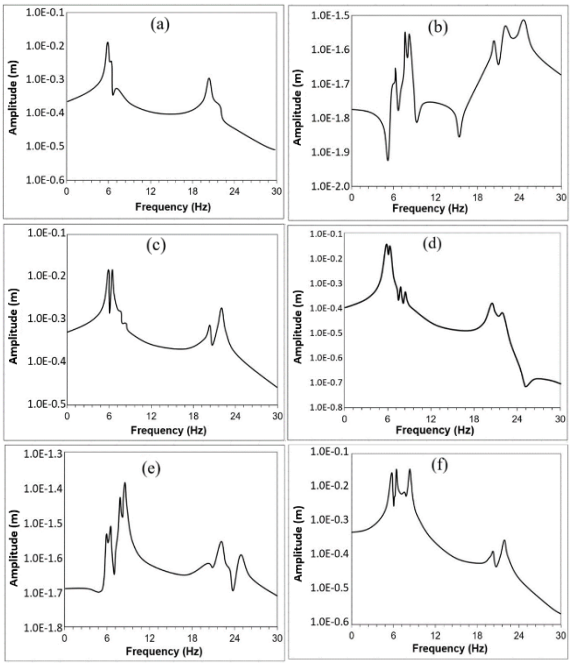

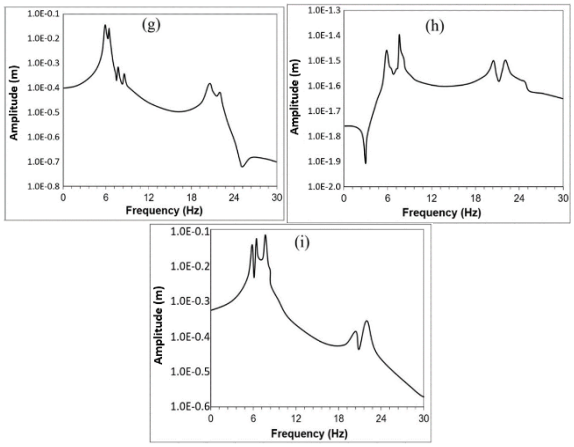

Figure 8. Frequency response of Raft: (a) Bounce (b) Roll (c) Pitch, Machine-1: (d) Bounce (e) Roll (f) Pitch and Machine-2: (g) Bounce (h) Roll (i) Pitch; when Machine-1 having excitation force (ANSYS).

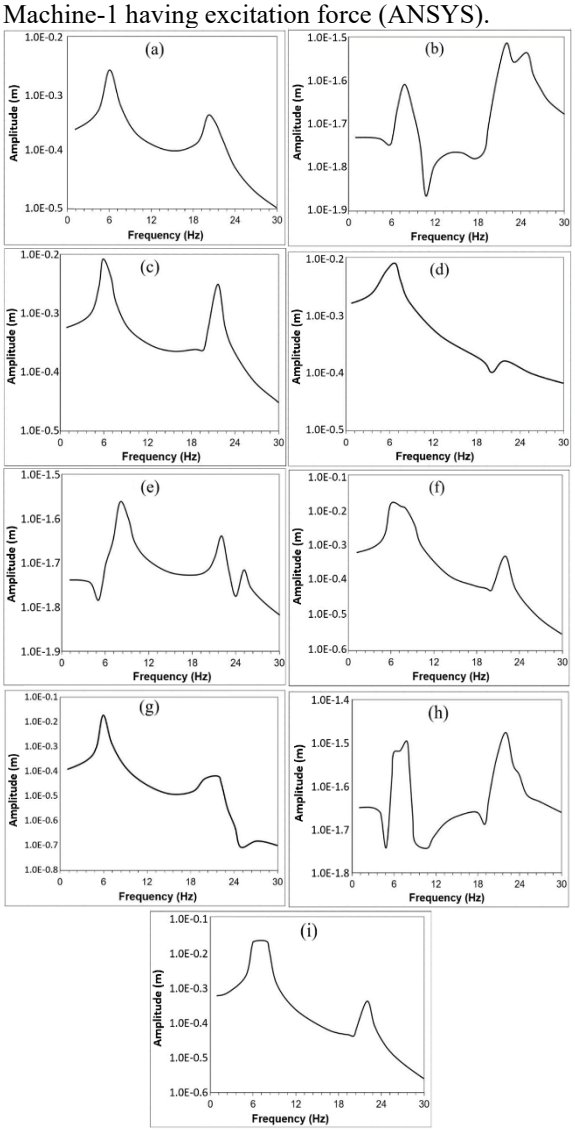

Figure 9. Frequency response of Raft: (a) Bounce (b) Roll (c) Pitch, Machine-1: (d) Bounce (e) Roll (f) Pitch and Machine-2: (g) Bounce (h) Roll (i) Pitch when; Machine-2 having excitation force (ANSYS).

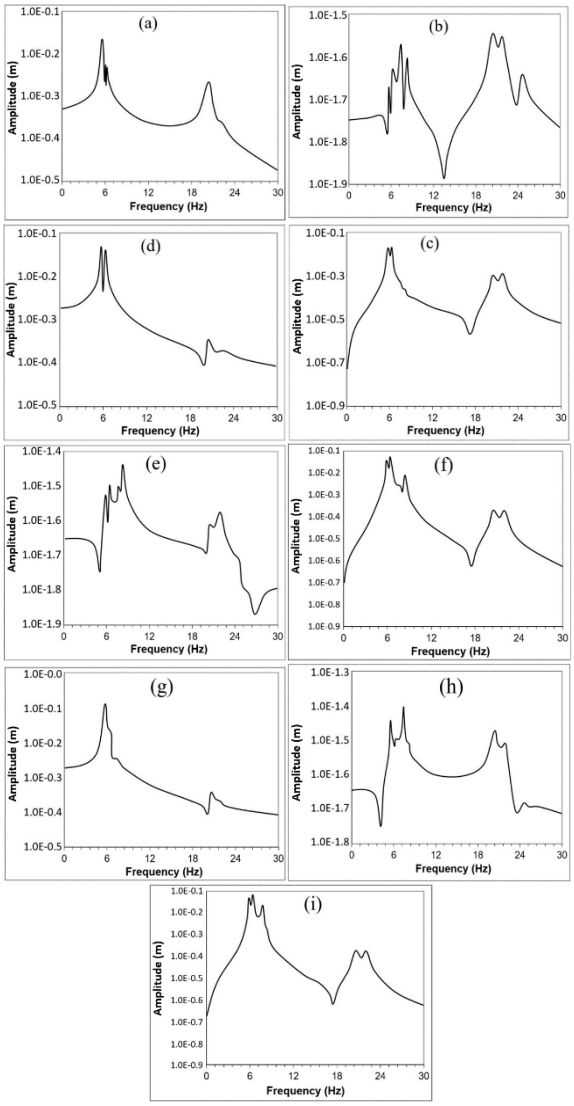

Figure 10. Frequency response of Raft: (a) Bounce (b) Roll (c) Pitch, Machine-1: (d) Bounce (e) Roll (f) Pitch and Machine-2: (g) Bounce (h) Roll (i) Pitch; when Machine-1 and Machine-2 having excitation force (ANSYS).

Maximum and minimum amplitudes at natural frequencies of the raft-mounted system are obtained corresponding to positive and negative force, respectively and values are listed in Table 7.

Table 7. Maximum and minimum amplitudes of raft mounting system at mode frequencies (ANSYS).

Mode Number	Maximum Displacement (m)	Minimum Displacement (m)
1	0.0298	-0.02484
2	0.0592	-0.06210
3	2.733×10^{-15}	-2.423×10^{-16}
4	0.0277	-0.01361
5	4.3772×10^{-15}	-7.101×10^{-15}
6	0.0317	-0.04040
7	0.0118	-0.06210
8	2.013×10^{-18}	-7.101×10^{-15}
9	0.0089	-0.04040

EXPERIMENTAL ANALYSIS

Experimental testing involves artificially exciting the structure with a specially designed impact hammer with an inbuilt piezo-sensor. The tip used to excite the structure is very specific for different structures; rubber tip can excite frequencies up to 500 Hz, plastic tip up to 1000 Hz and steel up to 5 kHz; choosing a suitable tip plays a vital role in proper excitation of the structure. Once the structure is suitably excited by the impact hammer, the responses, i.e., structural vibration due to it, are acquired using an accelerometer. The output of the sensors is recorded in the FFT analyser. These received signals are processed to get the frequency response function (FRF). The block diagram of the test method is shown in Figure 11.

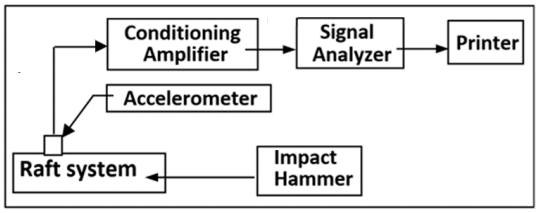

Figure 11. Block diagram of impact hammers test method.

The experiment utilizes a comprehensive instrumentation setup, including a LAN-XI data collector and analyzer (type 3050-A-060) with a 51.2 kHz frequency range and Type 2831-A battery module, supported by Pulse Software (Type 7700) for FFT, CPB (1/n-octave), and overall level analysis, capable of simultaneous measurement of exponential, linear, impulse, and peak levels. An impact hammer (8208 B&K type) with 0.23 mV/N sensitivity and a measuring range of 22,100 is used, along with a piezoelectric accelerometer (10.13 mV/m/s² sensitivity, 0–10 kHz frequency range), Nexus power amplifier, Microdot cable, and a display unit. The experimental setup, shown in Figure 12, features a rigidly fixed foundation connected to a raft through a two-stage mounting system: the first stage links the foundation to the raft, and the second stage connects the raft to the machine. The impact hammer test procedure follows this setup to evaluate system responses effectively.

The experimental set-up is placed on the foundation, fixed to the ground with hexagonal nuts and bolts. Accelerometers are placed on the raft and machines that generate an electric charge when mechanically stressed or compressed due to the vibration induced by the raft and machines. The raft and machines are set into vibration with force generated by hitting with the impact hammer

individually. The electric signal proportional to the acceleration is generated within the accelerometer, which forms the input to the conditioning amplifier. Condition amplifier amplifies the signal produced with a specific gain set into the system. The output from the conditioning amplifier is fed into the signal analyzer to convert the analogue signal for time to frequency domain conversion. The output is windowed in the range of interest (0-200 Hz) as our modal frequencies are within the limit. The output is the plot between frequency vs. acceleration at the X-axis and Y-axis, respectively. The foundation is rigidly fixed on the floor with hexagonal nuts and bolts. It is excited by an impact hammer (having built-in sensors to measure the applied force) on the foundation's outer surface. Simultaneously, response is measured with accelerometers at the excitation point. The measured force and response signal is processed to get the FRF (Frequency Response Function) and phase which gives the modal frequencies of the foundation. The frequency domain acceleration response of machine 1, machine 2, and raft obtained from the experimental test is shown in Figure 13.

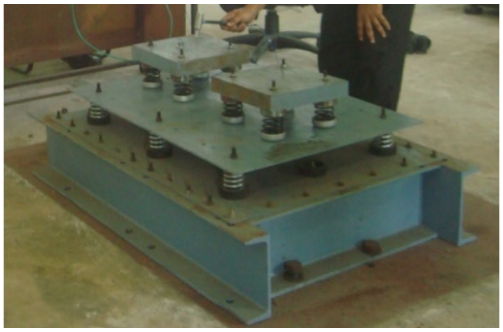

Figure 12. Experimental setup.

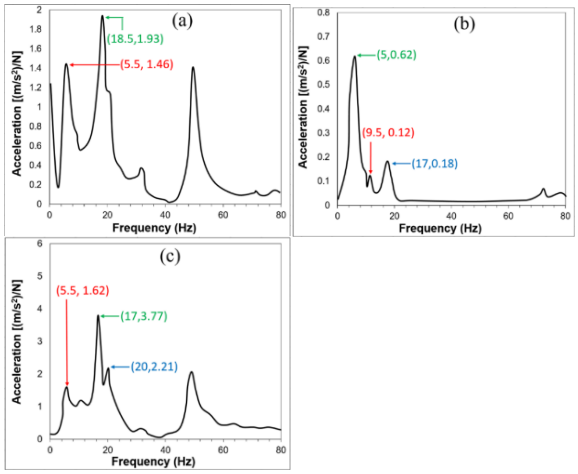

Figure 13. Frequency domain acceleration response of (a) machine 1, (b) machine 2, (c) raft (Experimental)

RESULTS & DISCUSSION

The modal analysis for raft mounting system is performed in ANSYS, MATLAB. The system's modal frequencies are obtained experimentally using the impact hammer method. The results are shown in Table 8, where natural frequencies obtained from MATLAB, ANSYS and experiment are denoted as f_{nM} , f_{nA}, and f_{nE} respectively; while % Error between MATLAB & ANSYS, MATLAB & Experiment, and ANSYS & Experiment are denoted as $\%Er(M-A)$, $\%Er(M-E)$, and $\%Er\,(A-E)$ respectively.

The results from MATLAB and ANSYS align closely due to accurate modeling assumptions. A little higher discrepancy between the simulated and experimental results highlights the real-world effects like imperfections in setup and environmental factors. Although ANSYS uses Finite Element Analysis (FEA), which is generally more precise due to its spatial discretization, errors persist. For example, the 4th mode has a 16.97% error. The errors could be due to mesh resolution or mesh density and the element type in ANSYS may not completely capture the system's dynamics. A refined mesh can be used for simulation with a higher hardware configuration in future which is a limitation at the time of carrying the work. Also, the experimental setup may have constraints or forces that differ slightly from those modeled. The larger error values (e.g., 19.07% for the 6th mode) indicate significant differences between the MATLAB simulations and experimental conditions. Factors like ambient disturbances, imperfect material properties, or non-uniform boundary conditions during the experiment can contribute to this error. Additionally, MATLAB calculations might have assumed ideal conditions (e.g., linear material behavior or perfect isotropy) that don't fully represent the experimental setup.

Table 8. MATLAB, ANSYS and Experimental natural frequencies and % Errors.

Mode No.	f_{nM} (Hz)	f_{nA} (Hz)	f_{nE} (Hz)	$\%Er_{M-A}$	$\%Er_{M-E}$	$\%Er_{A-E}$
1	5.924	5.9069	5.0	0.29	15.60	15.35
2	6.459	6.4554	5.5	0.06	14.85	14.80
3	8.420	8.4200	9.5	0.456	12.81	12.82
4	20.49	20475	17	0.077	17.03	16.97
5	22.02	22.01	18.50	0.032	15.99	15.96
6	24.71	24.71	20	0.0084	19.07	19.07

* f_{nM} , f_{nA}, and f_{nE} denote Natural frequencies obtained from MATLAB, Ansys, and Experiment respectively. $\%Er_{M-A}$, $\%Er_{M-E}$, and $\%Er_{A-E}$ denote percentage Error between Matlab & Ansys, between Matlab & Experiment, and between Ansys & Experiment respectively.

Table 9. Values of M-1, M-2 and Raft response in Harmonic analysis from ANSYS and MATLAB.

Mode no.	Mode shape	Displacement response in ANSYS (m)	Displacement response in MATLAB (m)	% Error
1	M1 B	0.0298	0.0297	0.3367
2	M2 B	0.0592	0.0590	0.3389
3	M1 R	2.733×10^{-15}	9.2490×10^{-17}	0.28
4	M1 P	0.0277	0.0227	0
5	M2 R	4.3772×10^{-15}	1.0383×10^{-17}	4.2
6	M2 P	0.0317	0.0317	0
7	Raft B	0.0118	0.0118	0
8	Raft P	2.013×10^{-18}	2.013×10^{-18}	0
9	Raft R	0.0089	0.0089	0

B: Bounce; R: Rolling; P: Pitching

Table 9 shows that the modal frequencies obtained from MATLAB and ANSYS are almost equal, and the maximum error obtained is about 0.456. It shows that the code developed for the system is acceptable. However, the results obtained from the experiment are comparable with the software results. The variation of results is due to the non-ideal conditions and the maximum error is 19%. The error is also due to external disturbances in the ambience which influence the results. Harmonic analysis for the raft mounting system is performed in the 0-30 Hz frequency range in ANSYS and MATLAB. The values of the response of harmonic analysis and the responses obtained from MATLAB and ANSYS are almost tallying, and the maximum error is 0.338%.

CONCLUSIONS AND FUTURE SCOPE

This study provides a framework for optimizing two-stage raft-mounted systems, supported by numerical and experimental analyses for improved vibration isolation. The equations of motion, derived via a matrix methodology, are applicable to systems with any number of isolators in arbitrary configurations. Using MATLAB and ANSYS, eigenvalues (natural frequencies) and eigenvectors (mode shapes) were calculated and validated against experimental modal testing, showing excellent agreement. Varying raft mass demonstrated its effect on natural frequencies. Forced vibration analysis under harmonic excitation also yielded consistent results between FEA and MATLAB, confirming the accuracy of harmonic response predictions.

Results revealed significantly reduced vibration responses for the two-stage system compared to single-stage systems, with displacement amplitudes as low as 0.0089 m at higher frequencies, demonstrating superior isolation. Recommendations include placing isolators near the center of mass and tuning stiffness to the system's natural frequencies to minimize resonance. These findings highlight the system's applicability in fields demanding strict vibration control, such as naval shipbuilding, precision manufacturing, and aerospace engineering.

REFERENCES

Al-Wakel, S.F., Fattah, M.Y., Karim, H.H., & Chan, A.H., Experimental and numerical modeling of machine foundations on a saturated soil. In *Numerical methods in geotechnical engineering*, CRC Press, Rotterdam, Netherland, pp. 1081-1086 (2015).

Barata, J., "Structures & Foundations Supporting Vibrating Machines," Master of Science Thesis, University of Lisbon (2019).

Evgeny, S., Oksana, I., Elena, Y., and Yuliya, V., "Mathematical modeling of vibration dampers of vibration insulated structures," EPJ Web of Conferences, Vol. 248 pp. 02009 (2021).

Guizani, A., Trabelsi, H., Abid, F. Hammadi, M., Barkallah, M., and Haddar, M., "New Approach for the Design and Optimization of a Quarter-Car Suspension System," Journal of the Chinese Institute of Engineers, Vol. 45, No. 7, pp. 579–587 (2022).

Jayarajan, P. and Kouzer, K.M., "Dynamic Analysis of Turbo-generator Machine Foundations,"; Journal of Civil Engineering and Environmental Technology, Vol. 1, No. 4, pp. 30-35 (2014).

Liu, L., Zuo, Z., Yau, J. D. and Urushadze, S., "A Simplified Method to Assess Vehicle–Bridge Interaction for Train-Induced Vibration of Light-Weight Railway Bridges," Journal of the Chinese Institute of Engineers, Vol. 45 No. (8), pp. 651–660 (2022).

Qiu, Y., Xu, W., Hu, Z., Zhang, S., "Model-based design of a novel modular mounting system: light, compact, and efficient," Advances in Mechanical Engineering, vol 14, no. 9 (2022).

Sharma, R.C., Palli, S., Sharma, S.K., "Ride analysis of railway vehicle considering rigidity and flexibility of the carbody," Journal of the Chinese Institute of Engineers, Vol. 46, No. 4, pp. 355-366 (2023).

Valliappan, S., and Hakam, A., "Finite element analysis for optimal design of foundations due to dynamic loading." International Journal for Numerical Methods in Engineering, vol 52, no. 5-6, pp. 605-614 (2001).

Xie, X., Zheng, S., Wang, S., & Zhang, Z., "Multi-degree-of-freedom ultra-low frequency vibration isolation system for precision devices with decoupled control", Measurement, vol. 237, no.115182 (2024),

Zhao, C., and Chen, D., "A two-stage floating raft isolation system featuring electrorheological damper with semi-active fuzzy sliding mode control," Journal of intelligent material systems and structures, vol. 19, no. 9, pp. 1041-1051 (2008).